ligand-based radical anion, and the solubility of the polymerized metal complex units.

(4) The polymerization efficiency, Φ_{poly}, approaches but never exceeds unity. This argues for hydrodimerization, and against a chain-growth mechanism, as the dominant pathway for monomer coupling.

(5) Charge-transport rates, film morphology, and dry-film conductivity measurements show the $((py)_2C_2)$-based films to be similar to other metallopolymer films prepared by EP but not to poly(acetylene).

Acknowledgment. The authors thank Professor Royce Murray and Dr. Pat Sullivan for their helpful comments. The experimental assistance of Dr. R. L. Jones with the SEM measurements is appreciated. Partial support for this work by the Office of Naval Research is gratefully acknowledged.

Registry No. TEAP, 2567-83-1; TBAH, 3109-63-5; vpy, 100-43-6; BPE, 13362-78-2; *cis*-$[Ru(bpy)_2((py)_2C_2)_2](PF_6)_2$, 97351-73-0; *cis*-$[Ru(bpy)_2(BPE)_2](PF_6)_2$, 97414-91-0; *mer*-$[Ru(trpy)((py)_2C_2)_3](PF_6)_2$, 97351-75-2; $[Ru(bpy)_2(vpy)_2]^{2+}$, 82769-08-2; $[Ru(bpy)_2(BPE)_2]^{2+}$, 97414-00-1; $[Ru(bpy)_2((py)_2C_2)_2]^{2+}$, 97351-72-9; $[Ru(trpy)(vpy)_3]^{2+}$, 83419-19-6; $[Ru(trpy)(BPE)_3]^{2+}$, 83082-73-9; $[Ru(trpy)((py)_2C_2)_3]^{2+}$, 97351-74-1; $[Ru(bpy)_2(vpy)_2]^{3+}$, 85661-74-1; $[Ru(bpy)_2(BPE)_2]^{3+}$, 97414-01-2; $[Ru(bpy)_2((py)_2C_2)]^{3+}$, 97351-76-3; $[Ru(trpy)(vpy)_3]^{3+}$, 85661-90-1; $[Ru(trpy)(BPE)_3]^{3+}$, 97414-02-3; $[Ru(trpy)((py)_2C_2)]^{3+}$, 97351-77-4; $[Ru(bpy)_2(vpy)_2]^{+}$, 97351-78-5; $[Ru(bpy)_2(BPE)_2]^{+}$, 97351-79-6; $[Ru(bpy)_2((py)_2C_2)]^{+}$, 97351-80-9; $[Ru(trpy)(vpy)_3]^{+}$, 97351-81-0; $[Ru(trpy)(BPE)_3]^{+}$, 97351-82-1; $[Ru(trpy)((py)_2C_2)]^{+}$, 97351-83-2; $[Ru(bpy)_2(vpy)_2]$, 97351-84-3; $[Ru(bpy)_2(BPE)_2]$, 97351-85-4; $[Ru(bpy)_2((py)_2C_2)]$, 97351-86-5; $[Ru(trpy)(vpy)_3]$, 97351-87-6; $[Ru(trpy)(BPE)_3]$, 97351-88-7; $[Ru(trpy)((py)_2C_2)]$, 97351-89-8; $[Ru(bpy)_2(vpy)_2]^{-}$, 97351-90-1; $[Ru(bpy)_2(BPE)_2]^{-}$, 97351-91-2; $[Ru(bpy)_2((py)_2C_2)]^{-}$, 97351-92-3; $[Ru(bpy)_2((py)_2C_2)]^{2-}$, 97351-93-4; *cis*-$Ru(bpy)_2Cl_2$, 19542-80-4; $(py)_2C_2$, 73564-69-9; Pt, 7440-06-4.

Contribution from the Department of Chemistry, Massachusetts Institute of Technology, Cambridge, Massachusetts 02139

Electrochemical Characterization of Surface-Bound Redox Polymers Derived from 1,1′-Bis[((3-(triethoxysilyl)propyl)amino)carbonyl]cobaltocenium: Charge Transport, Anion Binding, and Use in Photoelectrochemical Hydrogen Generation

RICHARD A. SIMON, THOMAS E. MALLOUK, KAREN A. DAUBE, and MARK S. WRIGHTON*

Received November 2, 1984

This paper describes the behavior of electrode-bound redox material derived from the hydrolysis of the $-Si(OEt)_3$ groups of 1,1′-bis[((3-(triethoxysilyl)propyl)amino)carbonyl]cobaltocenium (I). Surfaces of the conventional electrodes SnO_2 and Pt derivatized with I have a reversible electrochemical response in H_2O/electrolyte; the $E^{\circ\prime}$ is pH independent at −0.62 V vs. SCE. The photoelectrochemical behavior of p-type Si photocathodes derivatized with I reveals that the photoreduction of the cobaltocenium derivative can be effected at an electrode potential ~500 mV more positive than on metallic electrodes, consistent with the known behavior of p-type Si photocathodes. When polymer from I is deposited on p-type Si and subsequently coated with a small amount of Rh or Pd ($\sim 10^{-7}$ mol/cm^2), the photoelectrochemical generation of H_2 is possible with 632.8-nm (~15 mW/cm^2) radiation and efficiencies in the vicinity of 2%. The polymer derived from I is more optically transparent and more durable at negative potentials than redox polymers derived from viologen monomers. Potential-step measurements and steady-state-current measurements for mediated redox processes show that the charge-transport rate for the polymer derived from I is about the same as for polymers from viologen monomers. As for other positively charged redox polymers, the material from I will electrostatically bind large transition-metal complex anions such as $IrCl_6^{2-/3-}$, $Fe(CN)_6^{3-/4-}$, and $Mo(CN)_8^{3-/4-}$. A quantitative study of the relative binding of Cl^- and $Fe(CN)_6^{3-}$ has been done; $\Delta H^\circ = +12 \pm 0.5$ kcal/mol, and $\Delta S^\circ = +52 \pm 2$ cal/(mol K). Thus, entropy drives the displacement of Cl^- by $Fe(CN)_6^{3-}$. The redox potential of the $Fe(CN)_6^{3-/4-}$ system is approximately 50 mV more negative in the polymer compared to the solution potential.

In this paper we describe the behavior of electrode surfaces functionalized with a derivatizing reagent based on the cobaltocenium cation, 1,1′-bis[((3-(triethoxysilyl)propyl)amino)-carbonyl]cobaltocenium (I). The electrode-bound polymer from

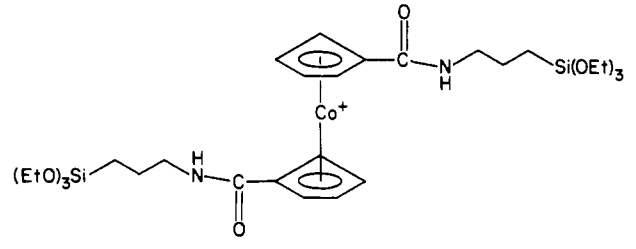

I

I is to be given the symbol $[(CoCpR_2^{+/0})_n]_{surf.}$. Our interest in a cobaltocenium-based polymer is due to the known durability and reversible redox properties of the cobaltocenium/cobaltocene couple.[1-3] To form a covalently anchored polymer based on I, the known chemistry of the $-Si(OEt)_3$ functionality is exploited via its reaction with H_2O and surface −OH groups.[4] Despite a considerable literature[5] on electrode-confined ferrocene reagents, there is only one report of the use of the cobaltocene system: the surface-confined cobaltocenium redox polymer poly(ethyleneimidocarbonylcobaltocenium) has been reported.[6]

The $[(CoCpR_2^{+/0})_n]_{surf.}$ system offers an attractive alternative to surface-confined viologen-based polymers[7-9] in photoelectro-

(1) Sheats, J. E. In "Organometallic Chemistry Reviews"; Seyferth, D., Ed.; Elsevier Scientific Publishing Co.: Amsterdam, 1979; p 461.
(2) Gubin, S. P.; Smirnova, S. A.; Denisovich, J. *J. Organomet. Chem.* **1971**, *30*, 257.
(3) Vlcek, A. A. *Collect. Czech. Chem. Commun.* **1965**, *30*, 952.
(4) Arkles, B. *CHEMTECH* **1977**, *7*, 766.
(5) (a) Wrighton, M. S.; Austin, R. G.; Bocarsly, A. B.; Bolts, J. M.; Haas, O.; Legg, K. D.; Nadjo, L.; Palazzotto, M. C. *J. Am. Chem. Soc.* **1978**, *100*, 1602. (b) Wrighton, M. S.; Palazzotto, M. C.; Bocarsly, A. B.; Bolts, J. M.; Fischer, A. B.; Nadjo, L. *J. Am. Chem. Soc.* **1978**, *100*, 7264. (c) Wrighton, M. S.; Austin, R. G.; Bocarsly, A. B.; Bolts, J. M.; Haas, O.; Legg, K. D.; Nadjo, L.; Palazzotto, M. C. *J. Electroanal. Chem. Interfacial Electrochem.* **1978**, *87*, 429. (d) Wrighton, M. S.; Bocarsly, A. B.; Bolts, J. M.; Bradley, M. G.; Fischer, A. B.; Lewis, N. S.; Palazzotto, M. C.; Walton, E. G. *Adv. Chem. Ser.* **1980**, *No. 184* 269. (e) Merz, A.; Bard, A. J. *J. Am. Chem. Soc.* **1978**, *100*, 3222. (f) Daum, P.; Murray, R. W. *J. Electroanal. Chem. Interfacial Electrochem.* **1979**, *103*, 289. (g) Chao, S.; Robbins, J. L.; Wrighton, M. S. *J. Am. Chem. Soc.* **1983**, *105*, 181.
(6) Roullier, L.; Waldner, E.; Laviron, E. *J. Electroanal. Chem. Interfacial Electrochem.* **1982**, *139*, 199.
(7) (a) Bookbinder, D. C.; Bruce, J. A.; Dominey, R. N.; Lewis, N. S.; Wrighton, M. S. *Proc. Natl. Acad. Sci. U.S.A.* **1980**, *77*, 6280. (b) Bruce, J. A.; Murahashi, T.; Wrighton, M. S. *J. Phys. Chem.* **1982**, *86*, 1552. (c) Bruce, J. A.; Wrighton, M. S. *Isr. J. Chem.* **1982**, *22*, 184. (d) Dominey, R. N.; Lewis, N. S.; Bruce, J. A.; Bookbinder, D. C.; Wrighton, M. S. *J. Am. Chem. Soc.* **1982**, *104*, 467.
(8) (a) Dominey, R. N.; Lewis, T. J.; Wrighton, M. S. *J. Phys. Chem.* **1983**, *87*, 5345. (b) Lewis, T. J.; White, H. S.; Wrighton, M. S. *J. Am. Chem. Soc.* **1984**, *106*, 6947.

0020-1669/85/1324-3119$01.50/0

chemical applications, most notably in the polymer-mediated reduction of solution species at illuminated p-type semiconductors. Polymers based on I are expected to admit a greater fraction of the incident light to the semiconductor than would equivalent thicknesses of viologen-based polymers, because of the much higher extinction coefficients of the latter in their singly reduced form.[8,10] In addition, $[(CoCpR_2^{+/0})_n]_{surf.}$ is expected to be durable in contact with aqueous solutions at potentials where the viologen-based polymers, in their doubly reduced state, degrade rapidly.[8]

The cobaltocenium/cobaltocene redox potential is generally much more negative than that of ferrocenium/ferrocene. But like the ferrocene system, there is a rich derivative chemistry of cobaltocene that makes the metallocenes attractive as electron-relay components in electrode-confined catalyst systems. The redox potential of $[(CoCpR_2^{+/0})_n]_{surf.}$ is close to that for the first reduction of the viologen-based polymers.[7-9] With respect to charge-transport properties, the Co(III/II) redox systems are expected, a priori, to have lower rates of charge transport in polymers than would the Fe(III/II) system of the ferrocenes, owing to the fact that the electron configurations are $3d^6/3d^7$ and $3d^5/3d^6$ for the Co(III/II) and Fe(III/II) systems, respectively. Interestingly, we find that the charge-transport properties of redox polymers derived from I compare favorably with the charge-transport properties of the viologen-based polymers[7,8,10] studied in this laboratory. Moreover, we find that the charge-transport properties of the polymers derived from I appear to be superior to those of the cobaltocenium-based polymer previously studied.[6] Additionally, since the $[(CoCpR_2^{+/0})_n]_{surf.}$ is covalently attached to the electrode surface, the use of large counterions in solution is not required for persistent attachment of the redox polymer, as is the case for the previously studied cobaltocenium-based polymer.[6]

Experimental Section

Synthesis of 1,1′-Bis(chlorocarbonyl)cobaltocenium. 1,1′-Dicarboxycobaltocenium as the PF_6^- salt[11,12] was refluxed in $SOCl_2$ for 2 days. The $SOCl_2$ was removed to yield a light green crystalline compound, which was washed with CH_2Cl_2 and dried in vacuo.

Elemental analysis of this compound (performed by Atlantic Microlabs, Inc., Atlanta, GA) was consistent with its formulation as a mixture of the PF_6^- and HCl_2^- salts of 1,1′-bis(chlorocarbonyl)cobaltocenium, as noted by Sheats and Rausch.[12] Anal. Calcd for 69% PF_6^-, 31% HCl_2^-: C, 33.2; H, 1.92; Cl, 22.0. Found: C, 32.9; H, 2.07; Cl, 22.0.

Synthesis of 1,1′-Bis[((3-(triethoxysilyl)propyl)amino)carbonyl]cobaltocenium (I) and Derivatization of Electrodes. I was generated in situ by combining 1,1′-bis(chlorocarbonyl)cobaltocenium (10 mg) with $(EtO)_3Si(CH_2)_3NH_2$ (15 μL) and Et_3N (10 μL) in 2 mL of dry CH_3CN. To this solution were added 5 mL of saturated aqueous KPF_6 solution and ~1.0 g of KCl. Pt electrodes and SnO_2-coated glass electrodes, fabricated and pretreated as described elsewhere,[7,8,10] were functionalized with I by holding them at −0.8 V vs. SCE in the degassed, quiet solution for periods of 10 min to 2 h. The electrodes were then held briefly at −0.2 V vs. SCE to reoxidize the polymer, dipped in distilled water, and "cured" in air at 100 °C for ~30 min. p-Si electrodes, fabricated and pretreated as previously described,[7] were held at ~−0.3 V vs. SCE under a 632.8-nm beam-expanded He–Ne laser (~50 mW/cm²) in the derivatizing solution for 30 min to 1 h. The potential was returned briefly to ~0.0 V vs. SCE in the dark, and the electrodes were dipped in distilled water and cured overnight, in vacuo, at ambient temperature.

Derivatization of electrodes could also be effected by soaking pretreated surfaces overnight in a ~5 mM solution of I generated in situ in CH_3CN; the solution was left open to the air. Polymer films prepared in this manner generally showed less uniformity of coverage than did those prepared by the electrochemically assisted deposition described above.

General Procedures and Instrumentation. Electrochemical data were obtained for N_2- or Ar-purged solutions by using a PAR Model 173 potentiostat and Model 175 voltage programmer or by using a Pine Instruments programmable bipotentiostat. Cyclic voltammograms and steady-state current–voltage curves were recorded with a Houston Instruments Model 2000 X-Y recorder. Electrochemical experiments were performed in a single-compartment cell with a saturated calomel reference (SCE) electrode, Pt counter electrode, and the appropriate working electrode. For rotating-disk-electrode experiments, the finished electrodes were mounted in the shaft of a variable-speed stirring motor from Polysciences, Inc. The rotation rate of the rotating disk electrode was determined by using a photodiode connected to a Power Instruments, Inc. tachometer. Pt rotating disk electrodes were typically coated with a ~3000-Å film of conducting indium tin oxide (ITO) by using a Materials Research Co. Model 8620 radio frequency sputtering system operating at ~200 W power output. A pressed powder ITO target was sputtered for ~30 min. The ITO coating provides a good surface onto which I can be anchored and suppresses H_2 evolution.

Absorption spectra were recorded on a HP 8451A diode array spectrophotometer. Spectroelectrochemical measurements on SnO_2 glass electrodes were made by using an electrochemical cell fitted with quartz windows. The SnO_2 was ~3400 Å thick. Illumination of p-Si was provided by an Aerotech Model LS5P 5-mW He–Ne laser. Auger spectra and depth profiles were obtained with a Physical Electronics Model 590A scanning Auger spectrometer.

Scheme I. Synthetic Procedure for the Preparation of I

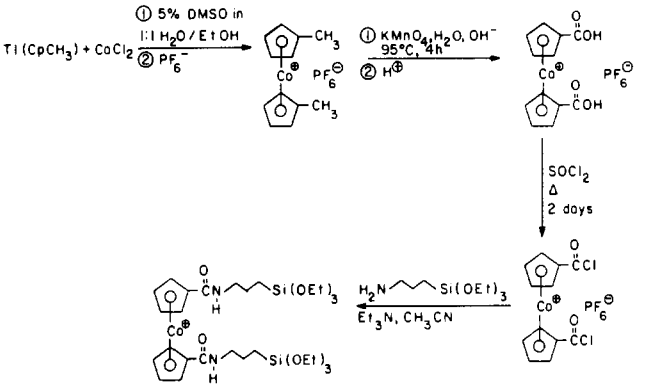

Results and Discussion

Characterization and Electrochemistry of Electrodes Derivatized with I. Compound I was synthesized by adaptation of a literature preparation, Scheme I.[11,12] I is generally formed in situ in the derivatizing solution by mixing 1,1′-bis(chlorocarbonyl)cobaltocenium, $(EtO)_3Si(CH_2)_3NH_2$, and Et_3N in CH_3CN. Pretreated electrode surfaces can be functionalized with I by soaking the electrode in ~5 mM I in CH_3CN. Functionalization of electrode surfaces can also be effected by electrochemically assisting the deposition of the polymer onto the electrode surface from an H_2O/CH_3CN solution that contains a high electrolyte concentration (cf. Experimental Section). Presumably, the reduction of I leads to deposition, because the reduced form is less soluble. Concentrating the monomer then leads to faster polymerization. Similar behavior has been found with viologen-based reagents bearing $-Si(OR)_3$ groups.[8,10]

Electrodes derivatized with I show a persistent electrochemical response in aqueous electrolyte solution. The cyclic voltammetry as a function of scan rate for a derivatized SnO_2 electrode, $SnO_2/[(CoCpR_2^{+/0})_n]_{surf.}$, in aqueous electrolyte solution is shown in Figure 1; the wave with a $E^{\circ\prime} \simeq 0.62 \pm 0.02$ V vs. SCE is attributed to the process represented by eq 1. The $E^{\circ\prime}$ value is

$$SnO_2/[(CoCpR_2^{+})_n]_{surf.} \underset{-ne^-}{\overset{ne^-}{\rightleftharpoons}} SnO_2/[(CoCpR_2^{0})_n]_{surf.} \quad (1)$$

independent of pH in the range of 0–10. The $E^{\circ\prime}$ value is taken to be the average position of the anodic and cathodic current peaks. The electrochemistry of I in 0.1 M KCl/H_2O solution exhibits well-defined cyclic voltammetry waves with $E^{\circ\prime} \simeq -0.68$ V vs. SCE, independent of pH. The surface-bound polymer from I thus has an $E^{\circ\prime}$ within ~60 mV of the solution analogue, as is expected in such comparisons.[13]

(9) (a) William, K. W.; Murray, R. W. *J. Electroanal. Chem. Interfacial Electrochem.* **1982**, *133*, 211. (b) Abruna, H. D.; Bard, A. J. *J. Am. Chem. Soc.* **1981**, *103*, 6898.
(10) Bookbinder, D. C.; Wrighton, M. S. *J. Electrochem. Soc.* **1983**, *130*, 1080.
(11) Sheats, J. E.; Kirsch, T. *Synth. Inorg. Met.-Org. Chem.* **1973**, *3*, 59.
(12) Sheats, J. E.; Rausch, M. D. *J. Org. Chem.* **1970**, *35*, 3245.
(13) Lenhard, J. R.; Rocklin, R.; Abruna, H.; William, K.; Kuo, K.; Nowak, R.; Murray, R. W. *J. Am. Chem. Soc.* **1978**, *100*, 5213.

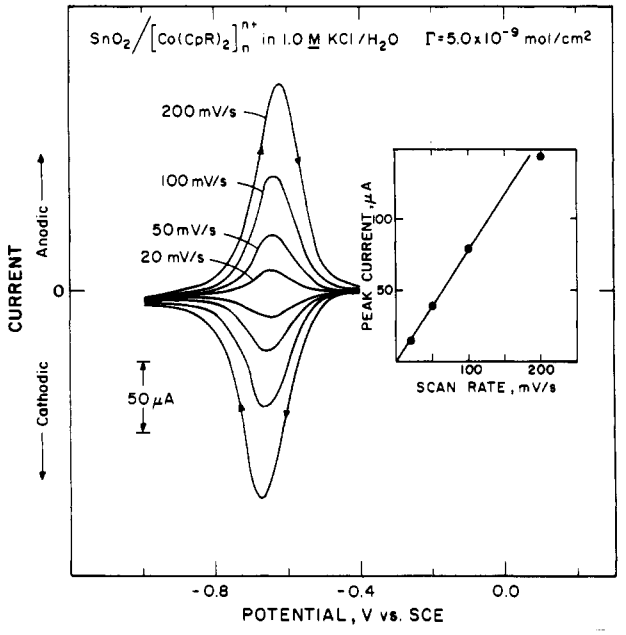

Figure 1. Cyclic voltammetry for $SnO_2/[(CoCpR_2^{+/0})_n]_{surf.}$ in 1.0 M KCl as a function of scan rate. Inset shows a plot of peak current vs. scan rate.

The surface-confined redox reagent from I can be repeatedly cycled through its oxidized and reduced form tens of thousands of times and held in its reduced form for prolonged periods of time, ≥48 h, in deoxygenated aqueous electrolyte solutions without significant loss of electroactive material and without deterioration in its properties. In comparison, the viologen-based polymer formed from *N,N'*-bis[3-(trimethoxysilyl)propyl]-4,4'-bipyridinium, $[(PQ^{2+/+/0})_n]_{surf.}$ on SnO_2 electrodes as described elsewhere,[7,8,10] was found to undergo rapid loss of electroactivity when cycled through the same potential range (−0.2 to −1.2 V vs. SCE) in degassed, 0.1 M aqueous KCl solution, Figure 2. Electrodes derivatized with I can be stored in air under ambient conditions for weeks without deterioration in the properties with respect to electrochemical responses.

The measurement of charge associated with the interconversion represented in eq 1 is used to determine the coverage of $CoCpR_2^{+/0}$ units per square centimeter of geometrical electrode area. Coverages as high as 1.5×10^{-7} mol/cm^2 have been obtained; assuming a monolayer is $\sim 10^{-10}$ mol/cm^2, this coverage corresponds to $>10^3$ monolayers. Typically, the reductive deposition of I yields more uniform films than does soaking the pretreated electrodes in a solution of I. Moreover, higher coverages can be obtained more rapidly and coverage can be controlled. Small areas (~25 μm^2) of electrodes derivatized with I show no surface morphology at ~500 Å by electron microscopy when I is deposited by using the electrochemical procedure. Thus, we regard the electrochemically assisted deposition as the procedure of choice for preparing derivatized electrodes with I.

Figure 3 illustrates UV–vis absorption spectral changes accompanying the interconversion represented by eq 1 for $[(CoCpR_2^{+/0})_n]_{surf.}$ deposited on optically transparent SnO_2 electrodes. For comparison, the figure also shows the optical properties of the oxidized and reduced solution species from reaction of *n*-$PrNH_2$ and 1,1'-bis(chlorocarbonyl)cobaltocenium, $CoCpR_2^{+/0}$. The oxidized solution species shows a visible maximum at 412 nm, $\epsilon \simeq 250$ M^{-1} cm^{-1}, consistent with the known spectrum of $CoCp_2^+$ itself.[14] The reduced species shows an absorption at 508 nm, $\epsilon \simeq 2100$ M^{-1} cm^{-1}. The spectroelectrochemical changes of $SnO_2/[(CoCpR_2^{+/0})_n]_{surf.}$ accord well with the spectroscopy of the solution species and show that the modified electrodes do not absorb intensely in the visible region of the spectrum.

(14) Sohn, Y. S.; Hendrickson, D. N.; Gray, H. B. *J. Am. Chem. Soc.* **1971**, *93*, 3603.

Electrostatic Binding of Complex Anions. Electrodes bearing $[(CoCpR_2^{+/0})_n]_{surf.}$ can firmly bind large anionic transition-metal complexes such as $Fe(CN)_6^{3-}$ and $Mo(CN)_8^{4-}$, Figure 4. The electrostatic binding of large electroactive anions to polycationic electrode-confined polymers has been previously demonstrated.[15] We have shown, for example, that when the electrodes bearing $[(CoCpR_2^+)_n]_{surf.}$ are soaked in 10 μM $Mo(CN)_8^{4-}$/0.1 M KCl solution for ca. 1 h, electrostatically bound $Mo(CN)_8^{4-}$ is present on the surface in an amount consistent with near-perfect charge compensation of the polymer. This conclusion is based on the charge passed in the $[(CoCpR_2^+)_n]_{surf} \rightleftarrows [(CoCpR_2^0)_n]_{surf.}$ interconversion compared to that for the $Mo(CN)_8^{3-} \rightleftarrows Mo(CN)_8^{4-}$ interconversion. The effect of the tightly bound anion on the reduction and oxidation of $[(CoCpR_2^{+/0})_n]_{surf.}$ is quite noticeable; the cyclic voltammetry waves tend to broaden, and the peak-to-peak separation increases. Of course, holding derivatized electrodes in the $[(CoCpR_2^0)_n]_{surf.}$ state leads to the extrusion of the bound anions.

Interestingly, the formal potential, $E^{\circ\prime}$, for the $Fe(CN)_6^{3-/4-}$ couple is at a more negative potential (+0.15 V vs. SCE at 25 °C) when the ion is bound in $[(CoCpR_2^{+/0})_n]_{surf.}$ compared to the $E^{\circ\prime}$ value in the same solution (0.1 M KCl/H_2O), +0.20 V vs. SCE. Apparently, in the solution, hydration and ion-pairing effects tend to stabilize the more highly charged $Fe(CN)_6^{4-}$ ion relative to $Fe(CN)_6^{3-}$, while in the polymer these effects are of less importance. There is a similar negative shift in $E^{\circ\prime}$ for $Mo(CN)_8^{3-/4-}$ (+0.52 V vs. SCE in $[(CoCpR_2^+)_n]_{surf.}$ vs. +0.58 V in solution).

Experiments have been done that establish the ordering of binding of anions to be $Mo(CN)_8^{4-} > Fe(CN)_6^{4-} \geq Fe(CN)_6^{3-} > IrCl_6^{2-} >> Cl^-$. Figure 4a illustrates the kind of experiment that was done to establish the ordering. The cyclic voltammetry of an electrode initially characterized as $[(CoCpR_2^+)_{n'}{}^1/_4nFe(CN)_6^{4-}]_{surf.}$ in 10 μM $Fe(CN)_6^{4-}$/10 μM $Mo(CN)_8^{4-}$/0.1 M KCl in H_2O changes to $[(CoCpR_2^+)_{n'}{}^1/_4nMo(CN)_8^{4-}]_{surf.}$ within 25 min. Figure 4b illustrates the cyclic voltammetry as a function of time for an electrode bearing $[(CoCpR_2^+)_{n'}nCl^-]_{surf.}$ equilibrated with 10 μM $Mo(CN)_8^{4-}$/0.1 M KCl in H_2O, showing essentially complete exchange of the Cl^- to give $[(CoCpR_2^+)_{n'}{}^1/_4nMo(CN)_8^{4-}]_{surf.}$ within 20 min. The ordering of binding of the transition-metal complexes is about the same as for other electrode-bound polycations studied in this laboratory.[16]

Some quantitative studies of the electrostatic binding of anions to electrode-bound polyanionic films have been made. In particular, the binding of electroactive cations in Nafion and in an organosilane–styrenesulfonate copolymer[18] has been examined quantitatively in terms of a partition coefficient, K_D, defined as the ratio of the concentration of the cation in the polymer to the concentration of the cation in solution. For Nafion/[(trimethylamino)methyl]ferrocene a single value of K_D obtains for all degrees of cation incorporation (including complete charge compensation) in the Nafion,[17] but for polysulfonate/$Ru(NH_3)_6^{2+}$ or methylviologen it was found that the value of K_D becomes smaller as the concentration of the cation is increased.[18] This kind of data can be useful in determining the thermodynamics for the competitive binding. We wish to illustrate that experimental measurements of the equilibrium constant for the anion exchange involving electrode-bound polymers from I can be made and that the temperature dependence gives valuable insight into the factors controlling the binding.

We adopted the formalisms used in describing ion exchange.[19,20]

(15) (a) Oyama, N.; Anson, F. C. *J. Electrochem. Soc.* **1980**, *127*, 247; *Anal. Chem. 1980, 52*, 1192. (b) Oyama, N.; Shimomura, T.; Shigehara, K.; Anson, F. C. *J. Electroanal. Chem. Interfacial Electrochem.* **1980**, *112*, 271. (c) Rubenstein, I.; Bard, A. J. *J. Am. Chem. Soc.* **1980**, *102*, 6641. (d) Shigehara, K.; Oyama, N.; Anson, F. C. *Inorg. Chem.* **1981**, *20*, 518. (e) Facci, J.; Murray, R. W. *J. Phys. Chem.* **1981**, *85*, 2870. (f) Kuo-Nam, K.; Murray, R. W. *J. Electrochem. Soc.* **1982**, *131*, 37. (g) Braun, H.; Storck, W.; Doblhofer, K. *J. Electrochem. Soc.* **1983**, *130*, 807.

(16) Bruce, J. A.; Wrighton, M. S. *J. Am. Chem. Soc.* **1982**, *104*, 74.

(17) Schneider, J. R.; Murray, R. W. *Anal. Chem.* **1982**, *54*, 1508.

(18) White, H. S.; Leddy, J.; Bard, A. J. *J. Am. Chem. Soc.* **1982**, *104*, 4811.

(19) Helfferich, F. "Ion Exchange"; McGraw-Hill: New York, 1962.

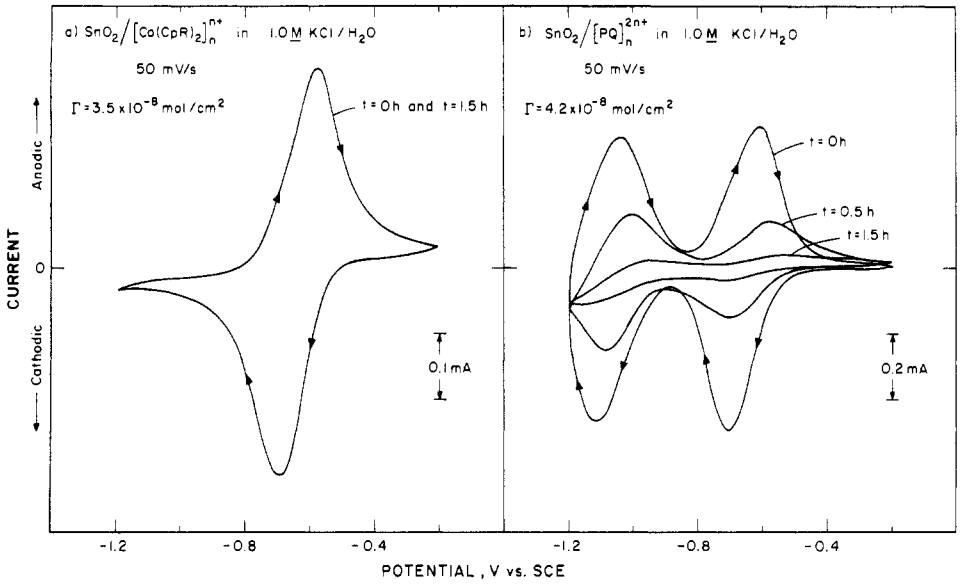

Figure 2. Cyclic voltammograms of $SnO_2/[(CoCpR_2^{+/0})_n]_{surf.}$ (a) and $SnO_2/[(PQ^{2+})_n]_{surf.}$ (b) as a function of time in 1.0 M KCl/H_2O, scan rate 50 mV/s. The decreasing area under the curves associated with $SnO_2/[(PQ^{2+})_n]$ after 0.5 and 1.5 h of repetitive cycling between +0.2 and −1.2 V is due to the irreversible decomposition of $[(PQ^0)_n]$ in H_2O. Notice that under the same conditions, $[(CoCpR_2^{+/0})_n]_{surf.}$ polymer is durable.

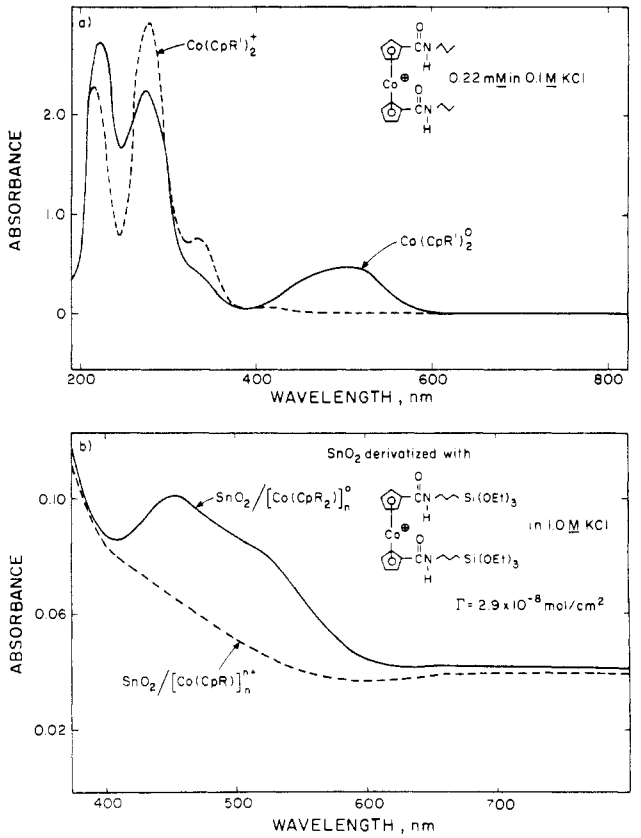

Figure 3. (a) UV–vis absorption spectra for 1,1′-bis[(*n*-propylamino)carbonyl]cobaltocenium (---) and 1,1′-bis[(*n*-propylamino)carbonyl]cobaltocene (—) in 0.1 M KCl/H_2O. (b) Visible absorption spectra for $SnO_2/[(CoCpR_2^{+/0})_n]_{surf.}$ in 1.0 M KCl/H_2O: (---) electrode potentiostated at 0.0 V vs. SCE; (—) electrode potentiostated at −0.8 V vs. SCE.

Consider the equilibrium involving anion A having a charge of z_A and anion B having a charge of z_B where A and B are in solution in equilibrium with a polycation (eq 2), where soln and polymer

$$z_B A_{soln} + z_A B_{polymer} \rightleftarrows z_A B_{soln} + z_B A_{polymer} \quad (2)$$

refer to species in the solution and polycation, respectively. For

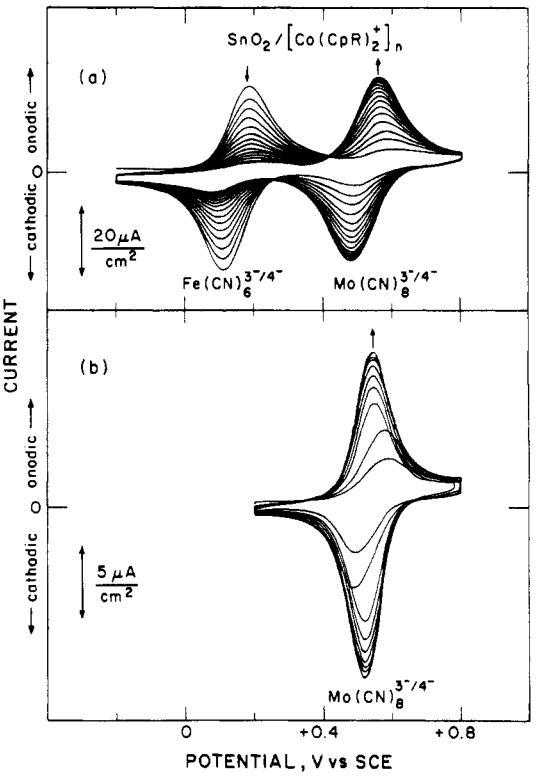

Figure 4. Cyclic voltammograms for (a) displacement of $Fe(CN)_6^{4-}$ by $Mo(CN)_8^{4-}$ in $[(CoCpR_2^{+/0})_n]_{surf.}$ (scan rate 20 mV/s) and (b) displacement of Cl^- by $Mo(CN)_8^{4-}$ in $[(CoCpR_2^{+/0})_n]_{surf.}$ (scan rate 10 mV/s).

such an equilibrium, the equilibrium constant, K_{eq}, is given by eq 3. In principle, the activity coefficients are extractable from

$$K_{eq} = \left(\frac{\bar{\gamma}_A \bar{C}_A}{\gamma_A C_A}\right)^{z_B}\left(\frac{\gamma_B C_B}{\bar{\gamma}_B \bar{C}_B}\right)^{z_A} = \left(\frac{\bar{\gamma}_A}{\gamma_A}\right)^{z_B}\left(\frac{\gamma_B}{\bar{\gamma}_B}\right)^{z_A}\left(\frac{\bar{C}_A}{C_A}\right)^{z_B}\left(\frac{C_B}{\bar{C}_B}\right)^{z_A} \quad (3)$$

$\bar{\gamma}_{A,B}$ ≡ activity coefficient of A,B in polymer
$\gamma_{A,B}$ ≡ activity coefficient of A,B in solution
$\bar{C}_{A,B}$ ≡ concentration of A,B in polymer
$C_{A,B}$ ≡ concentration of A,B in solution

(20) Buck, R. P. In "Ion-Selective Electrodes in Analytical Chemistry"; Freiser, H., Ed.; Plenum Press: New York, 1978; Vol. 1.

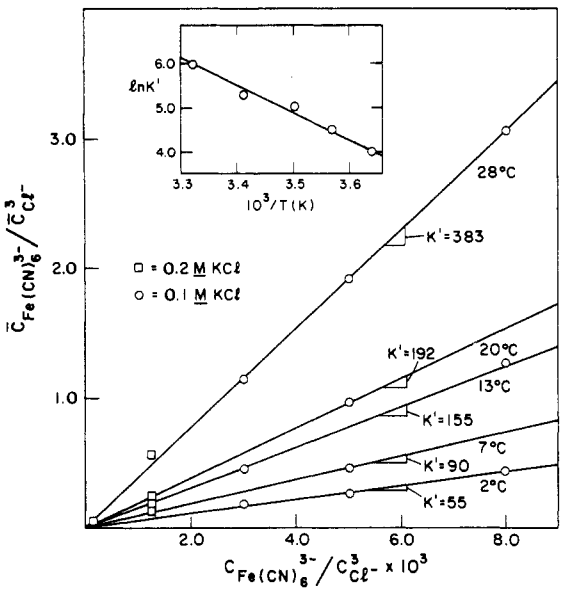

Figure 5. Ion-exchange isotherms for $Fe(CN)_6^{3-}/Cl^-$ in $[(CoCpR_2^{+/0})_n]_{surf.}$. K' is defined in eq 4.

the experimentally observed concentrations.[21] However, if the activity coefficients are invariant over the concentration range studied, an equilibrium constant, K', can be defined in terms of concentrations only (eq 4). We shall see that experiment justifies the use of eq 4.

$$K' = \left(\frac{\bar{C}_A}{C_A}\right)^{z_B}\left(\frac{C_B}{\bar{C}_B}\right)^{z_A} \quad (4)$$

Detailed experiments have been carried out for $[(CoCpR_2^{+})_n]_{surf.}$ as the electrode-bound polymer and the anions Cl^- and $Fe(CN)_6^{3-}$ (eq 5). Figure 5 shows that a plot of $\bar{C}_{Fe(CN)_6^{3-}}/\bar{C}_{Cl^-}^3$ vs.

$$Fe(CN)_6^{3-}{}_{soln} + 3Cl^-{}_{polymer} \rightleftarrows 3Cl^-{}_{soln} + Fe(CN)_6^{3-}{}_{polymer} \quad (5)$$

$C_{Fe(CN)_6^{3-}}/C_{Cl^-}^3$ is a straight line, as expected from eq 4. The linearity of the plots establishes that the ratio of activity coefficients in eq 3 is invariant with changes in concentration. The slope of the plot in Figure 5 thus gives K', and the data have been obtained at five temperatures in the range 2–28 °C. The inset in Figure 5 is a plot of ln K' vs. $1/T$; a straight line as expected for a temperature-independent $\Delta H°$. The slope gives a value of $\Delta H° = 12 \pm 0.5$ kcal/mol. Since the reaction proceeds from left to right under standard conditions, $\Delta G°$ must be negative. Thus, the positive $\Delta H°$ and the large temperature dependence on K' require that $\Delta S°$ be large and positive. Assuming that the ratio of activities is about 1, i.e. $K_{eq} \approx K'$, the intercept of the plot of ln K' vs. $1/T$ gives $\Delta S° = +52 \pm 2$ cal/(mol K). The large positive entropy change for the exchange reaction can be explained only in part by the release of three Cl^- from the polymer, since the standard entropy of the latter is 13.2 cal/(mol K) in aqueous solution.[22] Ion pairing between K^+ and $Fe(CN)_6^{3-}$ in solution occurs substantially in 0.1–0.2 M solutions of K^+ but cannot be invoked to explain the observed $\Delta H°$ and $\Delta S°$ for eq 5, since the pairing is entropy driven and weakly endothermic.[23] Strong hydration of $Fe(CN)_6^{3-}$ and $KFe(CN)_6^{2-}$, with concomitant ordering of the first hydration sphere, is probably lost to some extent in the polymer and may contribute positively to $\Delta H°$ and $\Delta S°$. Similar temperature-dependent behavior indicating a large positive $\Delta H°$ and $\Delta S°$ is qualitatively observed for the $Mo(CN)_8^{4-}/Cl^-$ and $Fe(CN)_6^{4-}/Cl^-$ exchange reactions. A more extensive study of the temperature dependence of ion binding involving other electrode-confined polymers will be carried out in this laboratory to test the generality of the large entropy factor in electrostatic binding of metal complexes.

Charge-Transfer Properties of $[(CoCpR_2^{+/0})_n]_{surf.}$. Cyclic voltammograms indicate that the $[(CoCpR_2^{+/0})_n]_{surf.}$ polymer can be rapidly reduced and oxidized. At low coverages, $\Gamma \leq 10^{-8}$ mol/cm^2, the peak current is directly proportional to the sweep rate up to ~200 mV/s. This suggests that the polymer possesses good redox kinetics that appear to be independent of any limiting factors up to a sweep rate of ~200 mV/s. At higher coverages, $\Gamma > 10^{-8}$ mol/cm^2, the peak current starts to become proportional to the square root of the sweep rate below 200 mV/s, indicating that the redox kinetics are limited by some sort of diffusional process. In other systems this diffusional process has been shown to be governed by the interplay of ion movement in and out of the polymer and by electron hopping between the immobilized redox centers.[24] At coverages of $\Gamma > 10^{-7}$, the cyclic voltammograms develop diffusion tails and the apparent coverage becomes a function of the scan rate; as the scan rate increases, the apparent coverage decreases. The electrolyte and its concentration clearly influence the charge transport within the $[(CoCpR_2^{+/0})_n]_{surf.}$ polymer; this can be seen by the shape of the cyclic voltammogram. At high coverages, increasing the electrolyte concentration from 0.1 to 1.0 M KCl results in cyclic voltammograms that possess sharper waves, a decrease in the diffusional tail, and a decrease in the separation of the cathodic and anodic current peak potentials. These effects suggest that the ionic strength and ion flux within the polymer play a role in determining the rate of charge transfer within the $[(CoCpR_2^{+/0})_n]_{surf.}$ polymer.

In order to study the steady-state current that can pass through the polymer, the reduction of $Ru(NH_3)_6^{3+}$ at rotating indium tin oxide (ITO) coated Pt-disk electrodes modified with I was studied. $Ru(NH_3)_6^{3+}$ was chosen because it does not appear to be able to penetrate through the $[(CoCpR_2^{+/0})_n]_{surf.}$ polymer, and the rate of reduction by the reduced polymer appears to be fast (eq 6).

$$[(CoCpR_2^{0})_n]_{surf.} + nRu(NH_3)_6^{3+} \xrightarrow{k_{et}} [(CoCpR_2^{+})_n]_{surf.} + nRu(NH_3)_6^{2+} \quad (6)$$

Evidence that $Ru(NH_3)_6^{3+}$ cannot penetrate $[(CoCpR_2^{+/0})_n]_{surf.}$ comes from the fact that the reduction current for the production of $Ru(NH_3)_6^{2+}$ onsets at the potential corresponding to the onset for the reduction of $[(CoCpR_2^{+/0})_n]_{surf.}$ and does not onset at the potential characteristic of naked Pt. The observed current, i_{obsd}, at a modified rotating disk electrode is controlled by the mass transport of $Ru(NH_3)_6^{3+}$ up to the electrode surface when the polymer is thin and/or the concentration of $Ru(NH_3)_6^{3+}$ is low. This conclusion comes from the strict linearity of the plot of limiting i_{obsd} vs. the square root of the rotation velocity, $\omega^{1/2}$,[25] when the electrode is held at a potential where the surface polymer is in the reduced state, ~−0.8 V vs. SCE, Figure 6. The fact that a mass-transport-limited reduction of 25 mM $Ru(NH_3)_6^{3+}$ can be effected at $\omega^{1/2} = 16$ rad$^{1/2}$/s$^{1/2}$ for an electrode with a coverage of 3.8×10^{-8} mol/cm^2 held at −0.8 V vs. SCE means that k_{et} is $>10^5$ M^{-1} s^{-1}. At higher coverages of $[(CoCpR_2^{+/0})_n]_{surf.}$ and/or higher concentrations of $Ru(NH_3)_6^{3+}$ the plots of limiting i_{obsd} vs. $\omega^{1/2}$ are nonlinear, Figure 6. $Ru(NH_3)_6^{3+}$ is no longer being reduced at a rate governed by mass transport but at a rate limited by the charge-transport rate through the $[(CoCpR_2^{+/0})_n]_{surf.}$ polymer.

When the observed state–state current, i_{obsd}, at a polymer-modified electrode is the polymer-limited current, i_E, eq 7 applies,

$$i_{obsd} = i_E = nFAD_{CT}C^2/\Gamma \quad (7)$$

where n is the number of electrons transferred per polymer redox center, F is Faraday's constant, A is the area of the electrode, D_{CT} is the diffusion constant for charge transport, C is the concentration of charge-carrier redox centers in the polymer, and Γ is the coverage of the polymer.[26] Equation 7 implies that the limiting

(21) Gaines, G. L.; Thomas, H. C. *J. Chem. Phys.* **1953**, *21*, 714.
(22) Latimer, W. M. "Oxidation Potentials", 2nd ed.; Prentice Hall: New York, 1952.
(23) Eaton, W. A.; George, P.; Hanania, G. I. H. *J. Phys. Chem.* **1967**, *71*, 2016.
(24) (a) Daum, P.; Murray, R. W. *J. Phys. Chem.* **1981**, *85*, 389. (b) Kaufman, F. B.; Engler, E. M. *J. Am. Chem. Soc.* **1979**, *101*, 547. (c) Peerce, P. J.; Bard, A. J. *J. Electron. Chem.* **1980**, *112*, 97.
(25) Galus, Z.; Adams, R. N. *J. Phys. Chem.* **1963**, *67*, 66.

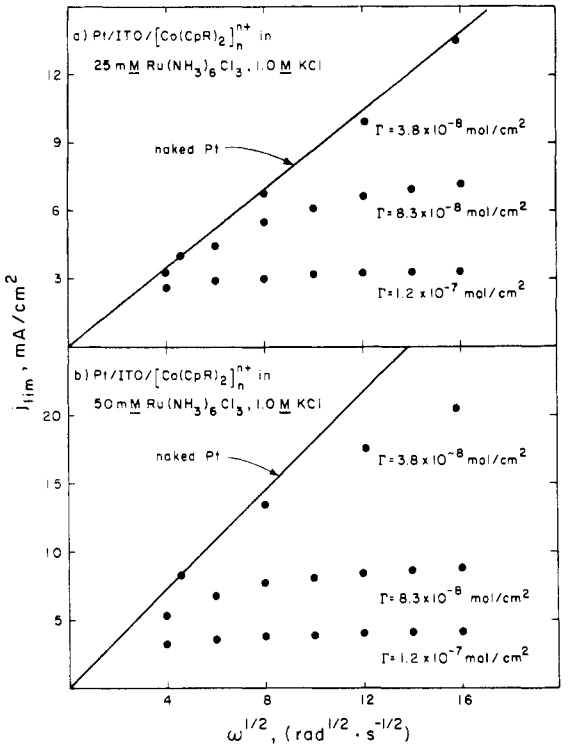

Figure 6. Levich plots, current density vs. $\omega^{1/2}$, for the reduction of (a) 25 mM and (b) 50 mM $Ru(NH_3)_6Cl_3$ at rotating Pt/ITO/$[(CoCpR_2^{+/0})_n]_{surf.}$ electrodes with various coverages in 1.0 M KCl/H_2O. The solid lines are the expected responses at naked Pt electrodes where mass-transport-limited reduction occurs.

current is a function of the polymer coverage. Figure 6a,b shows the plots of limiting i_{obsd} vs. $\omega^{1/2}$ for electrodes of various coverages, $\Gamma = 3.8 \times 10^{-8}$, 8.5×10^{-8}, and 1.2×10^{-7} mol/cm^2, used for the reduction of 25 and 50 mM $Ru(NH_3)_6^{3+}$. The limiting i_{obsd} is measured at −0.8 V vs. SCE where the polymer is in its fully reduced form. For the highest coverage the value of i_{obsd} is essentially independent of $\omega^{1/2}$, and it would appear that eq 7 applies. For the lower coverages the value of i_{obsd} is dependent on both $\omega^{1/2}$ and the value of i_E. This is a situation where eq 8 should give the relationship among the values of i_{obsd}, i_E, the kinetic limited current (i_k) (governed by k_{et}), and the mass-transport-limited current (i_L).[27] The value of K in eq 8 is the equilibrium constant for the polymer-mediated process represented by eq 6. Since the value of K is large, eq 8 simplifies to eq 9. This is the literature

$$\frac{1}{i_{obsd}} = \frac{1}{i_L} + \frac{1}{i_E} + \frac{1}{i_k} + \left(\frac{1}{K} - 1\right)\frac{i_{obsd}}{i_E i_L} \quad (8)$$

$$\frac{1}{i_{obsd}} = \frac{1}{i_L} + \frac{1}{i_E} + \frac{1}{i_k} - \frac{i_{obsd}}{i_E i_L} \quad (9)$$

equation that corresponds to the situation of a polymer-mediated redox reaction when the solution species does not penetrate the polymer.[27] The data points in all of the plots in Figure 6 are best fit with a $D_{CT}C^2$ value of 1×10^{-14} mol^2/(s cm^4) with an i_k value of ~4000 mA/cm^2 at 50 mM $Ru(NH_3)_6^{3+}$.[28] The estimated error in $D_{CT}C^2$ is ±15%. Two independent measures of $D_{CT}C^2$ have been obtained for $[(CoCpR_2^{+/0})_n]_{surf.}$ from the scan-rate dependence of the peak current in a linear-sweep voltammogram and potential-step chronoamperometry. Both of these techniques

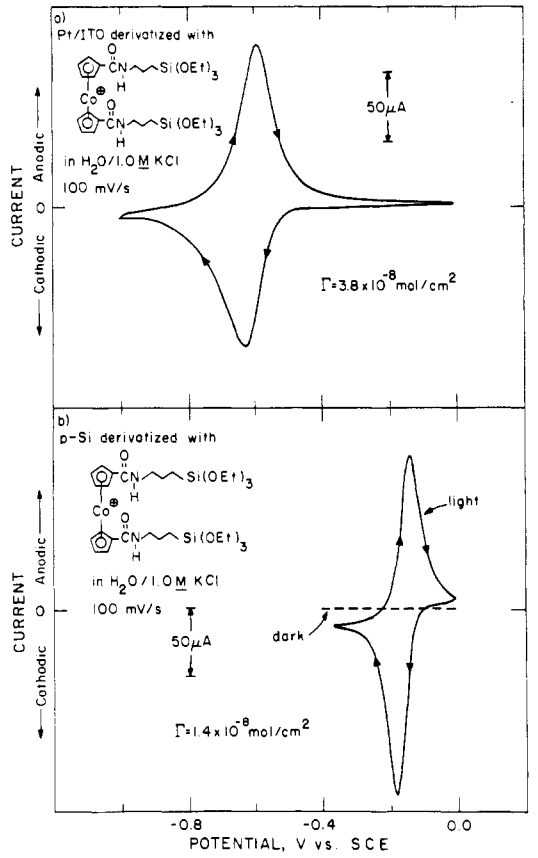

Figure 7. Cyclic voltammetric comparison of $[(CoCpR_2^{+/0})_n]_{surf.}$ on (a) SnO_2 and (b) p-Si in H_2O/1.0 M KCl at a scan rate of 100 mV/s. Illumination of p-Si with 632.8-nm light results in a reduction peak ~440 mV more positive than that for SnO_2; this is a measure of the photovoltage.

yield $D_{CT}C^2$ values within 10% of 1×10^{-14} mol^2/(s cm^4). Assuming that the value of C for $[(CoCpR_2^{+/0})_n]_{surf.}$ is 2 M, the value of D_{CT} is $\sim 2.5 \times 10^{-9}$ cm^2/s. This value of D_{CT} is about the same as that for the $[(PQ^{2+/+})_n]_{surf.}$ system previously reported.[7,8,10]

Photoelectrochemical Behavior of $[(CoCpR_2^{+/0})_n]_{surf.}$ and H_2 Generation. The $[(CoCpR_2^{+/0})_n]_{surf.}$ system has $E^{o\prime}$ and D_{CT} values that are similar to the values for the viologen-based polymers previously used as electron-relay systems on photocathode surfaces.[7-9] The better durability and optical properties of the $[(CoCpR_2^{+/0})_n]_{surf.}$ system compared to those of the viologen systems suggest that the $[(CoCpR_2^{+/0})_n]_{surf.}$ system would be a superior electron-relay system for mediated photoreduction processes such as H_2 evolution,[7] CO_3H^- reduction,[29] or reduction of biological substances requiring fast, outer-sphere mediators.[30] Here we wish to demonstrate that $[(CoCpR_2^{+/0})_n]_{surf.}$ can be anchored onto p-Si photocathodes and that interfaces as represented in Scheme II can be fabricated and can function as catalytic photoelectrodes for H_2 evolution.

Figure 7 shows a comparison of the cyclic voltammetry of $[(CoCpR_2^{+/0})_n]_{surf.}$ on Pt/ITO and 632.8 nm (~50mW/cm^2) illuminated p-Si. As expected, the reduction of $[(CoCpR_2^{+/0})_n]_{surf.}$ can be effected at a more positive electrode potential on the illuminated p-Si than on a metallic electrode. The extent to which the reduction is more positive is at best ~500 mV under the illumination conditions used; this is one measure of the photovoltage from the photocathode. This photovoltage is about what is expected for p-Si in contact with a redox reagent having an $E^{o\prime}$ of −0.62 V vs. SCE.[31] The pH-independent $E^{o\prime}$ of

(26) Pickup, P. G.; Murray, R. W. *J. Am. Chem. Soc.* **1983**, *105*, 4510.
(27) (a) Andrieux, C. P.; Saveant, J. M. *J. Electroanal. Chem. Interfacial Electrochem.* **1982**, *134*, 163; *Ibid.* **1982**, *142*, 1. (b) Anson, F. C.; Saveant, J. M.; Shigehara, K. *J. Phys. Chem.* **1983**, *87*, 214. (c) Anson, F. C.; Saveant, J. M.; Shigehara, K. *J. Am. Chem. Soc.* **1983**, *105*, 1096. (d) Harrison, D. J.; Wrighton, M. S. *J. Phys. Chem.* **1984**, *88*, 3932.
(28) This value was determined by measuring $k_{et} \simeq 8 \times 10^6$ M^{-1} s^{-1}, by using cobaltocenium polymer modified rotating microelectrodes, in experiments to be described elsewhere: Mallouk, T. E.; Cammarata, V.; Crayston, J. A.; Wrighton, M. S., in preparation.
(29) Chao, S.; Stalder, C. J.; Summers, D. P.; Wrighton, M. S. *J. Am. Chem. Soc.* **1984**, *106*, 2723.
(30) Lewis, N. S.; Wrighton, M. S. *Science (Washington, D.C.)* **1981**, *211*, 944.
(31) Bocarsly, A. B.; Bookbinder, D. C.; Dominey, R. N.; Lewis, N. S.; Wrighton, M. S. *J. Am. Chem. Soc.* **1980**, *102*, 3683.

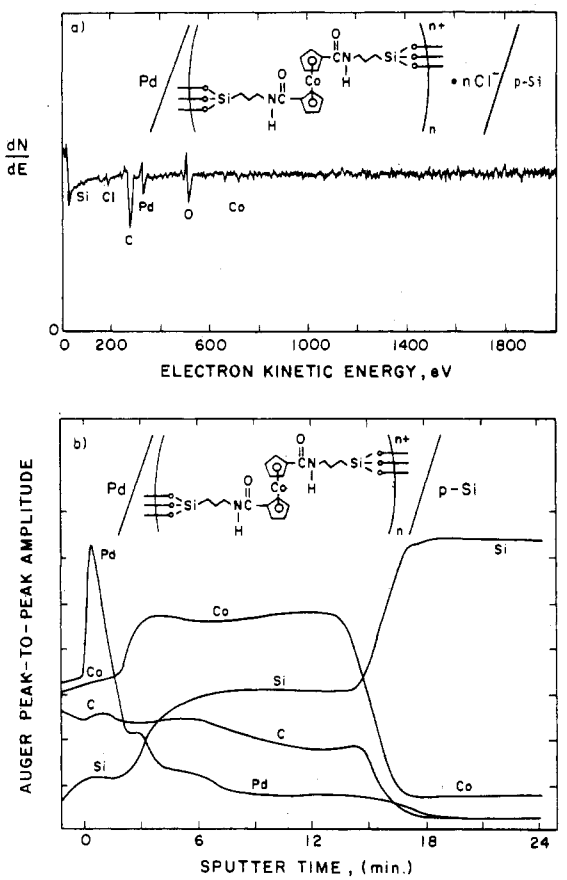

Figure 8. Auger analysis of the p-Si/$[(CoCpR_2^{+/0})_n]_{surf.}$/Pd interface: (a) Auger spectrum of modified electrode surface; (b) Auger depth profile of p-Si/$[(CoCpR_2^{+/0})_n]_{surf.}$/Pd.

$[(CoCpR_2^{+/0})_n]_{surf.}$ is more negative than $E^{\circ\prime}(H^+/H_2)$ for pH <6.3. This means that reaction according to eq 10 is spontaneous

$$[(CoCpR_2^0)_n]_{surf.} + nH^+_{aq} \rightarrow [(CoCpR_2^+)_n]_{surf.} + {}^1/_2nH_2 \quad (10)$$

for pH <6.3. Thus, p-Si electrodes derivatized with I should be capable of driving the production of H_2 with a photovoltage of

Scheme II. Interface for H_2 Generation

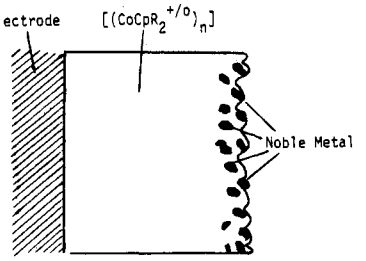

up to ~500 mV. But like the viologen-based electron relay[7] and other one-electron, outer-sphere reductants, the $[(CoCpR_2^0)_n]_{surf.}$ system does not react with H^+_{aq} at a significant rate. The evidence for a slow rate is that the photoreduction of $[(CoCpR_2^+)_n]_{surf.}$ on p-Si (Figure 7) shows little or no steady-state current at electrode potentials more negative than the potential where all of the polymer is in the reduced state. Thus, the reaction represented by eq 10 requires catalysis. Accordingly, interfaces like that represented by Scheme II have been fabricated where the role of the noble metal, M = Pd or Rh, is to equilibrate $[(CoCpR_2^{+/0})_n]_{surf.}$ with H^+/H_2.

An interface as shown in Scheme II has the feature that the noble metal is at the outermost portion of the polymer. Therefore, the only mechanism for charge transport to the catalyst sites is via charge transport through the polymer. Direct equilibration of the catalyst particles with the photogenerated reducing equivalents is not possible because the particles do not directly contact the p-Si. The method of synthesis for the interface in Scheme II is to hold the electrode at a potential and illumination intensity where the polymer is in its fully reduced state. Then, a reducible noble-metal precursor, e.g. $PdCl_4^{2-}$, is added at low concentration. The noble metal is then deposited onto the outermost portion of the polymer.[7] An Auger spectrum, run while sputtering with Ar^+ ions is taking place, establishes that the synthetic methodology works, Figure 8. The so-called depth-profile analysis given in Figure 8 shows that the noble metal is restricted to the outermost portion of the polymer. Structuring the catalyst assembly in this way has the advantage of giving a uniform, reproducible p-Si/polymer interface with a good photovoltage. Additionally, H_2 evolution will occur only at the outermost portion of the polymer so that mechanical disruption due to gas bubbles will be minimized compared to disruption in

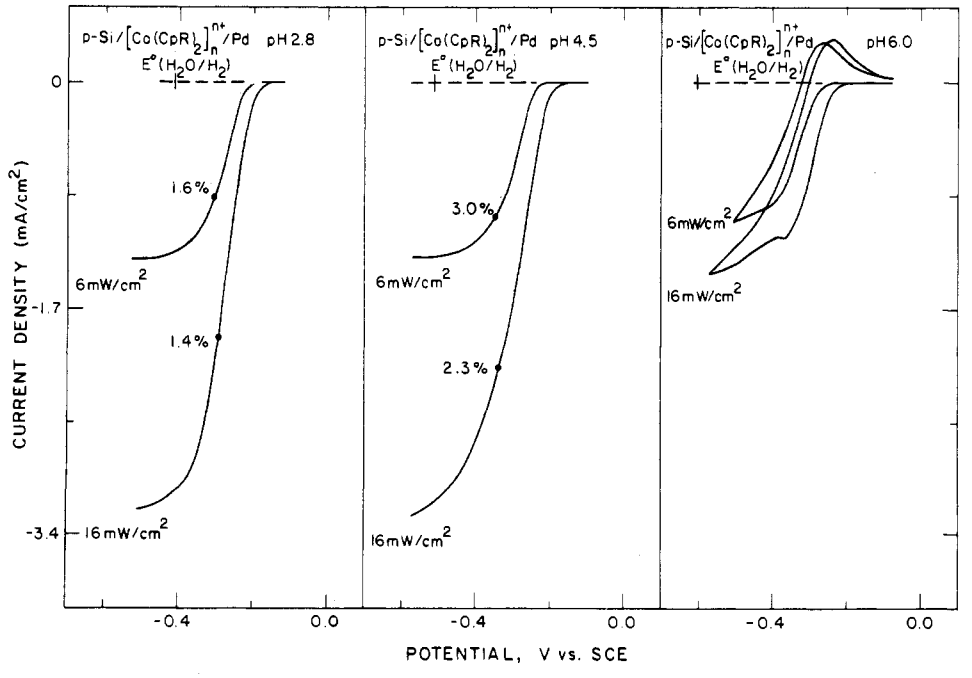

Figure 9. Steady-state (10 mV/s) photocurrent–voltage curves for a p-Si/$[(CoCpR_2^{+/0})_n]_{surf.}$/Pd electrode as a function of pH. The excitation source is a He–Ne laser (632.8 nm) at the indicated power density.

a catalyst structure where the noble metal is uniformly distributed throughout the polymer. Interfaces like that in Scheme II have also been fabricated by using Rh as the noble metal with aqueous $Rh_2(SO_4)_3$ as the reducible precursor.

The photoelectrochemical performance of a typical p-Si/$[CoCpR_2^{+/0})_n]/Pd_{surf.}$ photocathode is shown in Figure 9. The steady-state photocurrent voltage curves are shown as a function of pH. Since the polymer has a pH-independent redox potential and $E°'(H^+/H_2)$ varies 59 mV/pH unit, there is an optimum pH for the photoelectrochemical generation of H_2: at high pH the reaction represented by eq 10 is not thermodynamically viable and at low pH the photovoltage is low. Note that the photovoltage, E_V, is measured by the extent to which H_2 generation (at 1 atm) can be effected at a more positive potential than $E°'(H^+/H_2)$. At pH ≈6.3, where the equilibrium constant for eq 10 would be about 1, the rate is too slow to give a large photocurrent, i_{photo}. Even at pH 6.0 (Figure 9), the driving force is insufficient to give a photocurrent that is proportional to light intensity. The efficiency is defined by eq 11. We find that the $[(CoCpR_2^{+/0})_n]$/Pd catalyst

$$\eta\ (\%) = \frac{E_V i_{photo}}{\text{input optical power}} \times 100\% \qquad (11)$$

gives its highest efficiency at pH ≈4.5. No serious attempt has been made to optimize efficiency with this system, but the efficiencies for 632.8-nm illumination are about as good as with equivalent coverage of the viologen-based electron-relay system on p-Si photocathodes.[7] The pH-dependence of the photoelectrochemical efficiency shown in Figure 9 is consistent with the structure of the interface. Collectively, these experiments show that the use of I as a derivatizing reagent for photocathodes is viable. Recent experiments with p-InP/$[(CoCpR_2^{+/0})_n]/Rh_{surf.}$ show that significantly higher efficiencies (~10% for 632.8-nm illumination) can be obtained. The details of the surface chemistry of InP will be reported elsewhere.[32]

Conclusions

The cobaltocenium reagent I is a viable electrode derivatizing reagent for metallic and semiconducting materials. Both redox levels of $[(CoCpR_2^{+/0})_n]_{surf.}$ are rugged in aqueous solution. The redox potential, charge-transport rate, and metal-complex binding properties are similar to those of the viologen-based reagents previously studied in this laboratory. However, the polymer from I is more optically transparent and more durable at negative electrode potentials compared to the viologen-based reagents. Structured H_2 evolution catalyst systems can be prepared by using I, and the photoelectrochemical behavior accords well with the structure of the catalyst assembly.

In this work with $[(CoCpR_2^{+/0})_n]_{surf.}$ we have shown that it is possible to gain quantitative thermodynamic information regarding charge-compensating anion-exchange processes. Interestingly, a detailed study of the $Cl^-/Fe(CN)_6^{3-}$ and $Cl^-/Mo(CN)_8^{4-}$ systems shows that the selective uptake of the metal complexes is endothermic, $\Delta H° = +12$ kcal/mol for the $Fe(CN)_6^{3-}$, but there is a large, positive entropy change driving the process. The generality of this result will be tested in future experimentation.

Acknowledgment. We thank the U.S. Department of Energy, Office of Basic Energy Sciences, Division of Chemical Sciences, for support of this research. Partial support from GTE Laboratories is also gratefully acknowledged.

Registry No. I, 97551-35-4; $IrCl_6^{2-}$, 16918-91-5; $IrCl_6^{3-}$, 14648-50-1; $Fe(CN)_6^{3-}$, 13408-62-3; $Fe(CN)_6^{4-}$, 13408-63-4; $Mo(CN)_8^{3-}$, 17845-99-7; $Mo(CN)_8^{4-}$, 17923-49-8; SnO_2, 18282-10-5; H_2O, 7732-18-5; H_2, 1333-74-0; Pt, 7440-06-4; Cl^-, 16887-00-6; Si, 7440-21-3.

(32) (a) Spool, A.; Daube, K. A.; Mallouk, T. E.; Belmont, J. A.; Wrighton, M. S., in preparation. (b) Cf. also: Daube, K. A.; Harrison, D. J.; Mallouk, T. E.; Ricco, A. J.; Chao, S.; Wrighton, M. S.; Hendrickson, W. A.; Drube, A. J. *J. Photochem.* **1985**, *29*, 71.

Contribution from the Department of Chemistry, Ball State University, Muncie, Indiana 47306

Relative Phosphorus Ligand Sizes from Cis:Trans Distributions of $W(CO)_4(L)(L')$ Products Obtained from the Reaction of $W(CO)_4(L)(py)$ with L′ (L and L′ = Phosphines), Reaction Kinetics, and Syntheses of Starting Materials

MELISSA L. BOYLES, DANIEL V. BROWN, DENNIS A. DRAKE, CHERYL K. HOSTETLER, CONSTANCE K. MAVES, and JOHN A. MOSBO*

Received February 4, 1985

The relative sizes of 12 phosphines (L′ = PMe_3, $PPhMe_2$, PEt_3, $P(n\text{-}Bu)_3$, PPh_2Me, PPh_2Et, PPh_3, $P(p\text{-}tol)_3$, $PPh_2(i\text{-}Pr)$, $PPh_2(t\text{-}Bu)$, PBz_3, or PCy_3) have been studied by determining cis:trans ratios of $W(CO)_4(L)(L')$ products obtained from reactions of $W(CO)_4(L)(py)$ complexes with L′ (L = $PPhMe_2$, PPh_2Et, or $P(p\text{-}tol)_3$). In general, a decrease in the cis:trans ratio was observed as the Tolman cone angle of L′ increased. Exceptions occurred with PEt_3 and $P(n\text{-}Bu)_3$, for which cone angles of 140–145°, rather than Tolman's value of 132°, would be consistent with the other ratio data. Kinetic studies of these reactions indicate that dissociative loss of pyridine is rate limiting. Also reported are the synthesis of $W(CO)_4(L)(py)$ from $W(CO)_4(py)_2$ and L and ^{31}P NMR data for 21 new $W(CO)_4(L)(L')$ complexes.

Introduction

That phosphorus ligand sizes affect reactions involving transition metals to which they are attached is well documented.[1] A classic example of the purposeful use of ligand interactions is the asymmetric hydrogenation of prochiral olefins by Rh(I) catalysts.[2]

In order to quantify ligand sizes, Tolman introduced the concept of cone angle, θ.[3] In general, it is defined as the apex angle of a right cylindrical cone centered 2.28 Å from the center of a phosphorus atom that just touches the van der Waals radii of the outermost atoms. For unsymmetrical ligands, Tolman suggested use of half-cone angles, $\theta/2$.[1] These are defined as the angles between the metal–phosphorus vector and the vector that just touches the van der Waals radii of the outermost atoms.

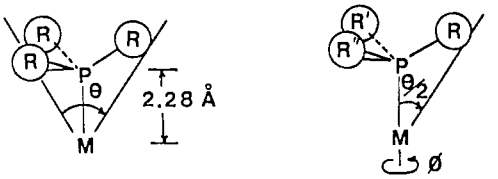

Phosphorus ligands have been assigned quantitative size values through three techniques based on the cone angle concept. Tolman has used CPK models,[1,3] some groups (particularly Alyea and Ferguson)[4] have utilized X-ray crystallographic data, and we have

(1) Tolman, C. A. *Chem. Rev.* **1977**, *77*, 313.
(2) See, for example: (a) Halpern, J. *Pure Appl. Chem.* **1983**, *55*, 99. (b) Knowles, W. S. *Acc. Chem. Res.* **1983**, *16*, 106.
(3) Tolman, C. A. *J. Am. Chem. Soc.* **1970**, *92*, 2956.

0020-1669/85/1324-3126$01.50/0